ISSN 1674-1056
http://cpb.iphy.ac.cn
http://iopscience.iop.org/cpb
中国物理 B
Chinese Physics
中国物理 Chinese Physics B

Structural transitions in $NaNH_2$ via recrystallization under high pressure

Yanping Huang(黄艳萍), Xiaoli Haung(黄晓丽), Xin Wang(王鑫), Wenting Zhang(张文亭), Di Zhou(周迪), Qiang Zhou(周强), Bingbing Liu(刘冰冰), Tian Cui(崔田)
Citation: Chin. Phys. B . 2019, 28(9): 096402 . **doi:** 10.1088/1674-1056/28/096402
Journal homepage: http://cpb.iphy.ac.cn; http://iopscience.iop.org/cpb

What follows is a list of articles you may be interested in

Semiconductor-metal transition in GaAs nanowires under high pressure

Yi-Lan Liang(梁艺蓝), Zhen Yao(姚震), Xue-Tong Yin(殷雪彤), Peng Wang(王鹏), Li-Xia Li(李利霞), Dong Pan(潘东), Hai-Yan Li(李海燕), Quan-Jun Li(李全军), Bing-Bing Liu(刘冰冰), Jian-Hua Zhao(赵建华)
Chin. Phys. B . 2019, 28(7): 076401 . **doi:** 10.1088/1674-1056/28/7/076401

Pressure-induced isostructural phase transition in α-$Ni(OH)_2$ nanowires

Xin Ma(马鑫), Zhi-Hui Li(李志慧), Xiao-Ling Jing(荆晓玲), Hong-Kai Gu(顾宏凯), Hui Tian(田辉), Qing Dong(董青), Peng Wang(王鹏), Ran Liu(刘然), Bo Liu(刘波), Quan-Jun Li(李全军), Zhen Yao(姚震), Bing-Bing Liu(刘冰冰)
Chin. Phys. B . 2019, 28(6): 066402 . **doi:** 10.1088/1674-1056/28/6/066402

Variational and diffusion Monte Carlo simulations of a hydrogen molecular ion in a spherical box

Xuehui Xiao(肖学会), Kuo Bao(包括), Youchun Wang(王友春), Hui Xie(谢慧), Defang Duan(段德芳), Fubo Tian(田夫波), Tian Cui(崔田)
Chin. Phys. B . 2019, 28(5): 056401 . **doi:** 10.1088/1674-1056/28/5/056401

Equation of state of $LiCoO_2$ under 30 GPa pressure

Yong-Qing Hu(户永清), Lun Xiong(熊伦), Xing-Quan Liu(刘兴泉), Hong-Yuan Zhao(赵红远), Guang-Tao Liu(刘广涛), Li-Gang Bai(白利刚), Wei-Ran Cui(崔巍然), Yu Gong(宫宇), Xiao-Dong Li(李晓东)
Chin. Phys. B . 2019, 28(1): 016402 . **doi:** 10.1088/1674-1056/28/1/016402

The effect of dislocations on the thermodynamic properties of Ta single crystal under high pressure by molecular dynamics simulation

Yalin Li(李亚林), Jun Cai(蔡军), Dan Mo(莫丹), Yandong Wang(王沿东)
Chin. Phys. B . 2018, 27(8): 086401 . **doi:** 10.1088/1674-1056/27/8/086401

Structural transitions in $NaNH_2$ via recrystallization under high pressure*

Yanping Huang(黄艳萍)†, Xiaoli Haung(黄晓丽)‡, Xin Wang(王鑫)§, Wenting Zhang(张文亭), Di Zhou(周迪), Qiang Zhou(周强), Bingbing Liu(刘冰冰), and Tian Cui(崔田)

College of Physics, State Key Laboratory of Superhard Materials, Jilin University, Changchun 130012, *China*

(Received 28 May 2019; revised manuscript received 10 July 2019; published online 30 August 2019)

Multiple phase transitions are detected in sodium amide ($NaNH_2$), an important hydrogen storage material, upon compression in diamond anvil cells (DAC) by using Raman spectroscopy and x-ray diffraction (XRD) measurements. Additional Bragg reflections appear on lower and higher angle sides of the original ones at $\sim$ 1.07 GPa and 1.84 GPa, accompanied by obvious changes in Raman spectroscopy, respectively. It reveals that $NaNH_2$ undergoes the high-pressure phase sequence (α–β–γ) up to 20 GPa at room temperature. Spectral analysis indicates an orthorhombic structure with *PBAN* space group for the γ phase. We also experimentally observe high pressure induced recrystallization in alkaline amide compounds for the first time.

Keywords: high pressure, sodium amide, phase transition, recrystallization

PACS: 64.60.–i, 07.35.+k, 61.05.cp, 78.30.–j **DOI:** 10.1088/1674-1056/ab37f8

1. Introduction

As a vitally important thermodynamic parameter, high pressure has been considered to be a crucial tool to research the intrinsic properties of materials.[1–9] New crystal structures and properties emerging through the application of high pressure also help interpret the elusive nature of novel phenomena or provide new routes for new materials. Recently, the great interest focusing on high pressure phase transitions of complex light-metal hydrides has been aroused based on a theoretical prediction of a new phase under high pressure by Vajeeston. The transition to a new high pressure $I4_1/a$ phase was predicted with a 17% volume collapse at about 2.6 GPa in $LiAlH_4$.[10] So they pointed out that it is worthwhile to investigate the reversibility and stabilization of high-pressure phases in those compounds, which have been predicted to exhibit superior hydrogen storage characteristics. If we can observe such a large volume collapse in experiment, and retain the high pressure phase to ambient pressure, then this would develop a new type of hydrogen storage material efficiently in aspect of gravity and volume. Interest in structural studies of these materials has therefore increased significantly during recent years.

There are many advantages of complex light-metal hydrides as the hydrogen storage material, such as high hydrogen content, relatively low decomposition temperature, environmental friendliness, and so on. Recently, there also has been significant interest in the properties of sodium amide ($NaNH_2$), although it has a relatively low theoretical hydrogen capacity (5.1 wt.%[11]) compared with its counterpart $LiNH_2$.[12] Nevertheless, it was proposed that $NaNH_2$ plays an important role in dehydrogenation with other light metal hydride systems when forming some composite hydrogen storage materials, for example, $NaNH_2$–$LiAlH_4$,[12] $NaNH_2$–MgH_2,[13] and $NaNH_2$–$LiBH_4$.[14] Structural properties of the ambient-condition phase of $NaNH_2$ (hereafter, α-$NaNH_2$) have been widely studied by x-ray and neutron diffraction experiments.[15,16] The α-$NaNH_2$ crystallizes into an orthorhombic phase belonging to space group $Fddd$ ($D224h$) with cell parameters $a = 8.964$ Å, $b = 10.456$ Å, $c = 8.073$ Å, and $Z = 16$.[17] However, the high-pressure behavior of $NaNH_2$ has not been extensively studied, especially the x-ray diffraction method is limited due to the weak scattering from the low-Z atoms. Recently, Liu *et al.*[18] observed two phase transitions at about 0.9 GPa and 2.0 GPa characterized by spectroscopical changes in both Raman and infrared (IR) experiments. Whereafter, the electronic structure and vibrational properties of $NaNH_2$ were calculated by Zhong[19] and two high pressure phases (orthorhombic, $P2_12_12$ and monoclinic, $C2/c$) were predicted by using the *ab initio* evolutionary structure prediction. However, no direct experimental evidence was reported, and detailed structural characterization of the high-pressure phases is extremely lacking.

The pressure-induced phase transitions in $NaNH_2$ have been observed through *in situ* high-pressure Raman spectra and synchrotron x-ray diffraction measurements up to 20 GPa

*Project supported by the National Key R&D Program of China (Grant Nos. 2018YFA0305900 and 2016YFB0201204), the National Natural Science Foundation of China (Grant Nos. 51632002, 51572108, 11504127, 91745203, and 11634004), Program for Changjiang Scholars and Innovative Research Team in University, China (Grant No. IRT_15R23), and National Fund for Fostering Talents of Basic Science, China (Grant No. J1103202).

†Corresponding author. E-mail: huangyp1124@jlu.edu.cn

‡Corresponding author. E-mail: huangxiaoli@jlu.edu.cn

§Corresponding author. E-mail: wang-xin@jlu.edu.cn

© 2019 Chinese Physical Society and IOP Publishing Ltd

at room temperature in this work. We observed interesting pressure-induced transformations and new phenomenon that have not been observed in the previous work. These high-pressure results may shed light on the lightweight hydrides.

2. Experimental methods

The air and moisture sensitive $NaNH_2$ powder (Alfa Aesar, purity $> 98\%$) was loaded with ruby chips into a Mao-type symmetric diamond anvil cell (DAC). The diamond culets used in DACs were 400 μm for both Raman and XRD experiments. A T301 stainless with a preindented 50-μm-thick was used as the gasket material, and a 100 μm sample chamber was created by a laser drilling system. To prevent the sample reacting with water, oxygen, and common pressure-transmitting media, no pressure medium was used, and the sample loading was performed in a glove box with inert N_2 atmosphere, which kept the O_2 and H_2O residual contents both below 0.1 ppm. The pressure inside the sample chamber was gauged at room temperature using the standard ruby fluorescence method,[20] the Raman ruby lines were sharp and well separated during the experimental pressure range. Thus, the quasi-hydrostatic conditions were confirmed to the highest pressure.

High-pressure angle-dispersive XRD measurements were carried out at 16-BM-D beamline of the High Pressure Collaborative Access Team (HPCAT) facility, at the Advanced Photon Source (APS), Argonne National Laboratory (ANL). The XRD experiments were performed at room temperature up to 20 GPa. The x-ray beam wavelength $\lambda = 0.3979$ Å. Diffraction images were obtained by a MAR3450 imaging plate detector, and then converted to XRD spectra (intensity versus 2θ patterns) through the FIT2D software.[21] The indexing and refinement of the XRD patterns were carried out by Material Studio software packages.[22] For the Raman experiment, we used a solid-state diode-pumped, frequency-doubled Nd: vanadate laser as the excitation laser, and the wavelength of the laser is 532 nm. In order to obtain high quality experimental data, we set the output power of the laser at 500 mW. The final Raman spectra were obtained through an ActonSpetraPro500i spectrograph with a liquid nitrogen cooled CCD detector (Princeton Instrument, 1340×100). All the Raman spectra were collected in the backscattering geometry.

3. Results and discussion

As Raman spectroscopy is a powerful tool to study the structural transitions through the investigations on the changes of the lattice and internal vibrational modes, the Raman spectra of $NaNH_2$ have been measured up to 20 GPa. The spectrum in the bottom of Fig. 1 was recorded near ambient conditions inside the closed DAC, and it showed good agreement with a reference spectrum which was recorded directly from the $NaNH_2$ powder. Figure 1(a) shows that the lattice modes are located in the low frequency region with nine resolved Raman peaks from 100 cm^{-1} to 600 cm^{-1}. Three expected peaks located at 1536 cm^{-1}, 3216 cm^{-1}, and 3267 cm^{-1} can be seen in Figs. 1(b) and 1(c) in the internal region, which are assigned to the bending mode ν_2, the symmetric N–H stretching mode ν_1, and the asymmetric N–H stretching mode ν_3,

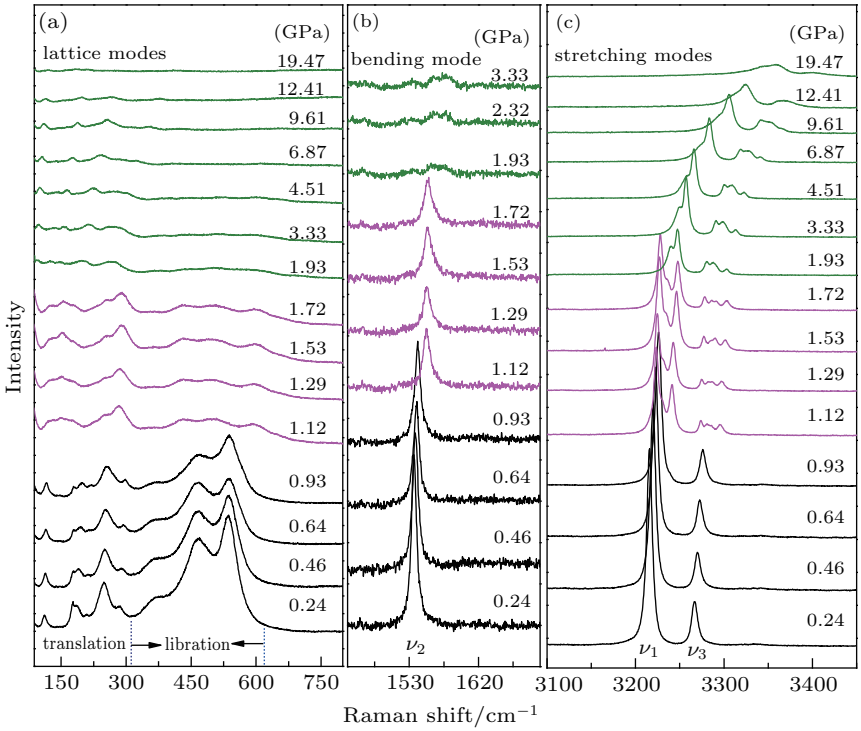


Fig. 1. Representative Raman spectra of $NaNH_2$ in the whole spectral regions upon compression at room temperature.

respectively.[18,23] Obviously, the Raman frequencies of all the internal modes of NH_2^{-1} are lower than those in $LiNH_2$,[24] indicating that the N–H distance in $NaNH_2$ is longer. Changes in the low-frequency region were observed by the abruptly weakened intensity for the librational modes during compression to 1.12 GPa. In addition, at 1.12 GPa, the ν_1 mode rapidly developed into a triplet and the ν_3 mode evolved into a tetrad as well. Such significant spectroscopic changes strongly suggest a phase transformation and a modification of the crystal structure from the initial phase at this pressure point, and the new phase is labeled as β-$NaNH_2$. Further compression to 1.93 GPa, the second phase transition from β- to γ-$NaNH_2$ was observed. During this structural transition, new lattice modes at lower frequencies were observed, and a marked decreased intensity for the H–N–H bending mode ν_2 together with splitting into a doublet was observed at 1.93 GPa, and entirely vanished beyond 3.33 GPa. Up to the highest pressure, all the Raman peaks became rather weak and broad, only the peak ν_1 mode was dominantly observable. The detailed pressure dependences of the measured Raman vibrational modes of $NaNH_2$ are shown up to 5.5 GPa in Fig. 2. In the region for the N–H symmetric and asymmetric stretching modes, all the modes show a strong upshift with pressure, and all the other modes exhibit slight pressure induced blue shifts. So there is no direct experimental evidence for the formation of hydrogen bonds either in the high pressure β- or γ-$NaNH_2$ phase from our Raman data.

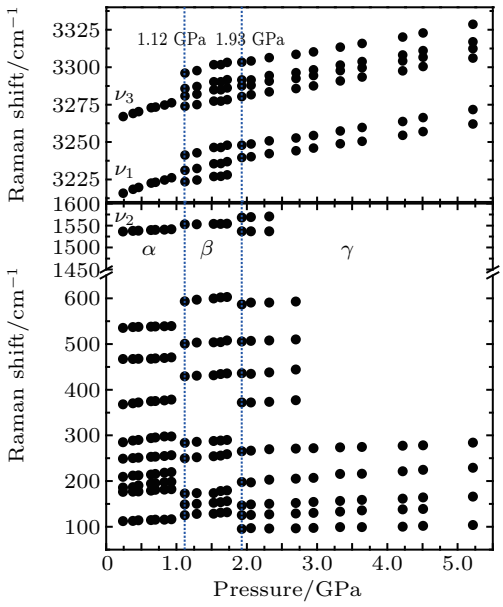


Fig. 2. The pressure dependence of vibration frequency for $NaNH_2$ up to 5.5 GPa. The phase boundaries are indicated by vertical dotted lines.

To corroborate our observations in the Raman spectra experiments and further determine the symmetry information of the new structures, *in situ* high pressure synchrotron XRD measurements have been carried out. At ambient condition, $NaNH_2$ has an orthorhombic symmetry with space group $Fddd$. Figure 3(a) shows the Rietveld refinement of $NaNH_2$ carried out on an XRD pattern obtained at 0.05 GPa. The Rietveld refinement of $NaNH_2$ shows an excellent agreement with the ambient structure, which is shown in Fig. 3(b). The Na atoms are located at the 16f positions, N at the 16g positions, and H at the 32f sites, and the structure contains NaN_4 tetrahedra with Na–N distances of 2.4–2.5 Å. The lattice constants obtained from the refined results are $a = 8.999$ Å, $b = 10.350$ Å, $c = 8.005$ Å with unit cell volume $V = 745.64$ Å^3, and they are in good accordance with those previously reported in the literature.[17]

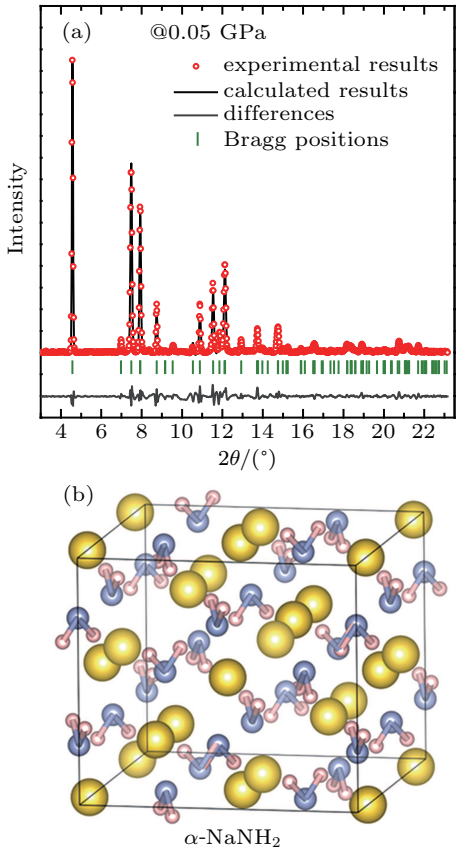


Fig. 3. (a) Powder x-ray diffraction pattern and Rietveld full-profile refinement of α-$NaNH_2$ structure at 0.05 GPa with $\lambda = 0.3979$ Å. The green vertical ticks indicate the expected Bragg positions and intensities of XRD peaks. (b) The crystal structures of α-$NaNH_2$. The yellow (largest), grey (medium), and pink (smallest) spheres represent sodium, nitrogen, and hydrogen atoms, respectively.

The pressure dependent powder XRD patterns of $NaNH_2$ taken at room temperature are shown in Fig. 4(a). At 0.05 GPa, all the diffraction peaks can be resolved to the ambient phase α-$NaNH_2$ by the Rietveld refinement. With increasing pressure, all the obtained diffraction peaks shift to larger angles, indicating the shrinkage of the lattice. With the increase of the pressure to 1.07 GPa, several new peaks appear indicating the appearance of the first phase transition, which is coincident with the Raman results of structure phase transition at 1.12 GPa. The shape, intensity, and width of the peaks of the β-$NaNH_2$ phase are distinct from those of the α-$NaNH_2$

phase. There are new peaks emerged at low and high angles in the XRD patterns, indicating that a first order-like structural transformation has taken place at this pressure point. With continuous compression to 2.25 GPa, the XRD diffraction peaks again exhibit distinct changes both in the numbers, intensities, and sharpness, coinciding with the Raman data from the β-$NaNH_2$ phase transition into the γ-$NaNH_2$ phase. Up to 16.52 GPa, the XRD patterns of the γ-$NaNH_2$ phase remain stable with weak and broadened peaks. During the whole compression process, we can provide experimental evidences for two structure phase transformations from α-$NaNH_2$ $\rightarrow$ β-$NaNH_2$ $\rightarrow$ γ-$NaNH_2$ by both the XRD patterns and Raman spectroscopy. When we release the pressure from the highest pressure to ambient pressure, the high pressure γ-$NaNH_2$ transforms back to α-$NaNH_2$ as shown in the top of Fig. 4(a), reflecting the reversible of the phase transitions. The XRD rings of the sample at different pressure points in Fig. 4(b) show that $NaNH_2$ reveals a recrystallization phenomenon under high pressure, which has not been observed in other alkaline amide compounds. The sample at 1.84 GPa shows much smoother diffraction rings than that at 0.05 GPa. Intriguingly, during the compression to 2.25 GPa, the sample begins to melt, and upon compression to higher pressure, the diffraction rings imply more uniform crystalline grains of $NaNH_2$ after the subsequent recrystallization, the melting phase reverts back to the crystalline phase.

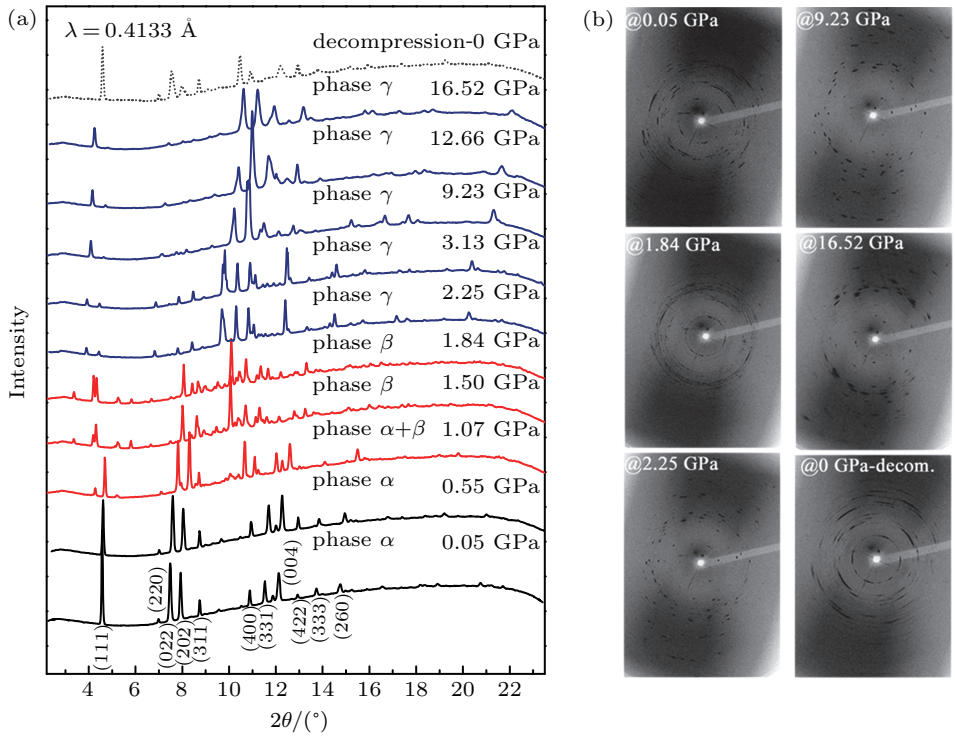


Fig. 4. (a) Representative angle dispersive x-ray diffraction patterns of $NaNH_2$ during compression to 16.52 GPa at room temperature. The Miller indexes (h k l) of the diffraction pattern peaks of ambient $NaNH_2$ phase are shown by the numbers under the first pattern. (b) The XRD rings of the sample at 0.05 GPa, 2.25 GPa, and 16.52 GPa respectively.

The present XRD results provide strong evidence of the two pressure-induced phase transitions in $NaNH_2$. We try to obtain more information of the crystal structures of β-$NaNH_2$ and γ-$NaNH_2$. Zhong *et al.* have predicted that the structures of β-$NaNH_2$ and γ-$NaNH_2$ are with the space groups $P2_12_12$ and $C2/c$, respectively.[19] Therefore, we firstly make comparison between our obtained experimental high pressure XRD patterns and the predicted crystal structures from the theoretical calculation by Zhong *et al.* However, both of their two structures do not match with our high pressure XRD patterns. Besides this, the energetically competing structures proposed by Zhong *et al.*, namely triclinic P-1, monoclinic $C2$, and orthorhombic $Amm2$ structures, are also considered for the high pressure structures of $NaNH_2$. Taken into the consideration of structural similarity with alkali metal amides, the tetragonal $LiNH_2$-type structure with I-4 space group and monoclinic KNH_2-type structure with $P2_1/m$ space group are also explored. However, all of these structures fail to match with our high pressure XRD patterns. To index the peaks belonging to the unknown compound, the obtained high pressure XRD data of the unknown phases are analyzed by the program DICVOL06[25] and PEAKFIT. For the β-$NaNH_2$ case, no indexing data can be resolved, probably because there are two phases mixed in β-$NaNH_2$. For phase γ, we select the data at 16.52 GPa to index, and the results show that it mainly belongs to an orthorhombic system. Several space groups are allowed for the orthorhombic system, for instance, *PBAN*, *P2AN*, *PB2N*, *PBMN*, and *PBA2*. Among them, *PBAN* is a

strong candidate for phase γ, because it is most appropriate for comparison with the diffraction profile at 16.52 GPa. The obtained lattice parameters from the fitting results of γ-$NaNH_2$ with *PBAN* space group at 16.52 GPa are $a = 8.4880$ Å, $b = 7.5655$ Å, and $c = 6.0678$ Å, which is shown in Fig. 5. The reason for such poor agreement with those structures predicted by theoretical investigation may be the presence of recrystallization during compression.

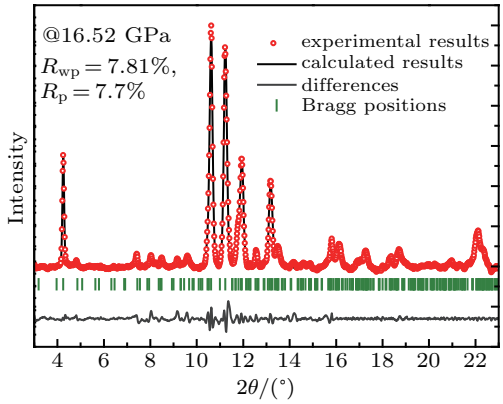


Fig. 5. The indexing of the XRD patterns of γ-$NaNH_2$ at 16.52 GPa.

4. Conclusion

A combination of synchrotron x-ray diffraction and Raman experiment has uncovered a complex sequence of phase transformation of $NaNH_2$ as a function of pressure. The ambient condition α-$NaNH_2$ first transforms into β-$NaNH_2$ at about 1 GPa and then into probably an orthorhombic γ-$NaNH_2$ with space group *PBAN* at about 2 GPa. Even though the intermolecular N–H distances become shortened during the compression process, all the vibrational modes exhibit blue shifts, so there is no hydrogen bonding effect within the pressure region. High pressure induced comminution and recrystallization may be the reason for the poor agreement with previous theoretical investigation.

Acknowledgements

The authors are grateful to Yue Meng and Jesse Smith for their technical support during the experiment. This work was performed at HPCAT (Sector 16), Advanced Photon Source (APS), Argonne National Laboratory. HPCAT operations are supported by DOE-NNSA under Award No. DE-NA0001974 and DOE-BES under Award No. DE-FG02-99ER45775, with partial instrumentation funding by NSF. The Advanced Photon Source is a US Department of Energy (DOE) Office of Science User Facility operated for the DOE Office of Science by Argonne National Laboratory under Contract No. DE-AC02-06CH11357.

References

[1] Mujica A, Rubio A, Muñoz A and Needs R J 2003 *Rev. Mod. Phys.* **75** 863
[2] Hemley R J and Ashcroft N W 1998 *Phys. Today* **51** 26
[3] Jayaraman A 1986 *Rev. Sci. Instrum.* **57** 1013
[4] Parise J B 2006 *Rev. Mineral. Geochem.* **63** 205
[5] Stoffler D 1997 *Science* **278** 1576
[6] Williams Q and Hemley R J 2001 *Annu. Rev. Earth Pl. Sc* **29** 365
[7] Mao H K, Chen X J, Yang D, Li B and Wang L 2018 *Rev. Mod. Phys.* **90** 15007
[8] Song T, Sun X W, Wei X P, Ouyang Y H, Zhang C L, Guo P and Zhao W 2019 *Acta Phys. Sin.* **68** 126201 (in Chinese)
[9] Sun J P, Prashant S, Zhou H X, Ni S L, Wang S H, Lei H C, Wang B S, Dong X L, Zhao Z X and Cheng J G 2018 *Acta Phys. Sin.* **67** 207404 (in Chinese)
[10] Vajeeston P, Ravindran P, Vidya R, Fjellvåg H and Kjekshus A 2003 *Phys. Rev. B* **68** 212101
[11] Ichikawa T, Isobe S and Kristallogr Z 2008 *Z. Kristallogr* **223** 660
[12] Xiong Z T, Hu J J, Wu G T, Liu Y F and Chen P 2007 *Catal. Today* **120** 287
[13] Sheppard D A, Paskevicius M and Buckley C E 2011 *J. Phys. Chem. C* **115** 8407
[14] Zhang Y and Tian Q 2011 *Int. J. Hydrogen Energy* **36** 9733
[15] Juza R, Weber H H and Opp K Z 1956 *Anorg. Allg. Chem.* **284** 73
[16] Nagib M, Kistrup H and Jacobs H 1975 *Atomkernenergie* **26** 87
[17] Zalkin A and Templeton D H 1956 *J. Phys. Chem.* **60** 821
[18] Liu A and Song Y 2011 *J. Phys. Chem. B* **115** 7
[19] Zhong Y, Zhou H Y, Hu C H, Wang D H and A Oganov A R 2012 *J. Phys. Chem. C* **116** 8387
[20] Mao H K, Xu J and Bell P M 1986 *J. Geophys. Res.* **91** 4673
[21] Hammersley A P, Svensson S O, Hanfl, M, Fitch A N and Häussermann D 1996 *High Press. Res.* **14** 235
[22] Jiao S H, Pang G S, Liang H W, Chen Y and Feng S H 2007 *J. Nanopart. Res.* **9** 605
[23] Cunningham P T and Maroni V A 1972 *J. Chem. Phys.* **57** 1415
[24] Chellappa R S and Chandra D 2007 *J. Phys. Chem. B* **111** 10785
[25] Boultif A and Louer D 2004 *J. Appl. Cryst.* **37** 724